Magnetic quantum correlations in the one-dimensional transverse-field XXZ model

Salimeh Mahdavifar,[1] Saeed Mahdavifar,[2,*] and R. Jafari[3,4,5,6,†]

[1]*Department of Physics, Alzahra University, 19834 Tehran, Iran*

[2]*Department of Physics, University of Guilan, 41335-1914 Rasht, Iran*

[3]*Department of Physics, Institute for Advanced Studies in Basic Sciences (IASBS), Zanjan 45137-66731, Iran*

[4]*School of Physics, Institute for Research in Fundamental Sciences (IPM), P.O.Box 19395-5531, Tehran, Iran*

[5]*Department of Physics, University of Gothenburg, SE 412 96 Gothenburg, Sweden*

[6]*Beijing Computational Science Research Center, Beijing 100094, China*

One-dimensional spin-$\frac{1}{2}$ systems are well-known candidates to study the quantum correlations between particles. In condensed matter physics, studies often are restricted to first-neighbor particles. In this work, we consider the one-dimensional XXZ model in a transverse magnetic field (TF) which is not integrable except at specific points. Analytical expressions for quantum correlations (entanglement and quantum discord) between spin pairs at any distance are obtained for both zero and finite temperature by using the analytical approach proposed by Caux *et al.* [Phys. Rev. B **68**, 134431 (2003)]. We compare the efficiency of the quantum discord (QD) with respect to the entanglement in the detection of critical points as the neighboring spin pairs go farther than the next-nearest neighbors. In the absence of the TF and at zero temperature, we show that the QD for spin pairs farther than the second neighbors is able to capture the critical points while the pairwise entanglement is absent. In contrast with the pairwise entanglement, two-site QD is effectively long range in the critical regimes where it decays algebraically with the distance between pairs. We also show that the thermal QD between neighbor spins possesses strong distinctive behavior at the critical point that can be seen at finite temperature and, therefore, spotlights the critical point while the entanglement fails in this task.

I. INTRODUCTION

Quantum phase transitions (QPTs) is one of the most interesting research topics in condensed-matter physics. It is a phase transition that theoretically occurs at absolute zero temperature where quantum fluctuations play the dominant role [1]. Due to suppression of the thermal fluctuations at zero temperature, the ground state of the system is introduced as the representative of the system which undergoes an abrupt change at the critical point (CP) [2]. The ground state's wave function of a many-body system near a CP at zero temperature is often nontrivial due to the long-range correlations among the system's constituents. Quantum correlations could be responsible for these correlations [3] and, consequently, could be useful for studying the QPT. Entanglement is a type of quantum correlation first pointed out by Schrödinger in 1935 [4] as the characteristic feature of quantum mechanics. It has been widely considered to be the main resource in most quantum information processing tasks [5–8]. However, in the past few years, it has been known that quantum correlations exist which are not spotlighted by entanglement measures. This is encompassed very efficiently in the formulation of so-called quantum discord (QD) as a measure to represent the broadness of quantum correlations [9,10]. Moreover, intimations exist that QD is the resource responsible for the speed up in deterministic quantum computation with one quantum bit [11,12]. Entanglement and QD have been studied extensively in a number of contexts, e.g., low-dimensional spin models [13–19], open quantum systems [20–24], biological systems [25], and relativistic [26,27] systems. Recently, pairwise QD and entanglement have been analyzed as a function of distance between spins in the transverse field XY chain for both zero- and finite-temperatures cases [18,28–30]. It has been displayed that, at zero temperature, QD can capture a QPT even for situations where entanglement is absent. Furthermore, pairwise QD of two nearest-neighbor spins in the XXZ model can also indicate the critical points for finite temperatures [15,31]. Indeed, establishing finite quantum correlations between distant parties is undoubtedly imperative to implement several quantum information processing tasks in many-body systems with short-range interactions. Along this direction, it has been shown that QD length is enhanced by introducing disorder in a spin chain while entanglement length is not [32].

In this paper we study pairwise entanglement and QD at both zero and finite temperatures in the one-dimensional (1D) XXZ chain in the presence of a transverse magnetic field which is not integrable except at specific points [33]. Our motivation is related to very recent studies of 1D many-body quantum systems of trapped ions [34,35] where the entanglement between pairwise spins in a one-dimensional quantum system of trapped ions has been observed [34]. Moreover, it is experimentally reported that constructed arrays of magnetic atoms on a surface can be designed to behave like spin-$\frac{1}{2}$ XXZ Heisenberg chains in a transverse magnetic field (TF) [35]. Consequently, the quantum correlation between different neighbor spins in the transverse field spin-$\frac{1}{2}$ XXZ Heisenberg chains can be measured experimentally. Furthermore, in Ref. [36], XXZ chains were used to describe quantum computers based on NMR and they can also be employed for solid-state quantum computers [37,38].

*smahdavifar@gmail.com

†rouhollah.jafari@physics.gu.se; rohollah.jafari@gmail.com

The main aim of this study is to search the behavior of the entanglement and QD at zero and finite temperature for spin pairs arbitrarily distant by using an analytical approach that combines a Jordan–Wigner transformation with a mean-field approximation [39]. To the best of our knowledge, such contributions have not been explored in previous works and can bring several new effects to the subject. We show that the QD for spin pairs more distant than nearest neighbors is able to characterize QPTs where pairwise entanglement is absent. This behavior is rather different from the behavior of two-spin entanglement, which is typically short range even in the critical regimes. Furthermore, an analysis displays that the entanglement and QD increase with magnetic field and temperature for certain regions of parameter space. We also show that the thermal QD is more robust than the thermal entanglement as the distance between the spin pairs is increased.

Then, it is constructive to review the main features of the one-dimensional XXZ chain in the presence and absence of a transverse magnetic field. The Hamiltonian of spin-$\frac{1}{2}$ XXZ Heisenberg chains in a TF is given by

$$\mathcal{H} = J \sum_{n=1}^{N} \left[S_n^x S_{n+1}^x + S_n^y S_{n+1}^y + \Delta S_n^z S_{n+1}^z \right], \qquad (1)$$

where S_n is the spin-$\frac{1}{2}$ operator of the nth site. $J > 0$ denotes the antiferromagnetic exchange coupling, and Δ is the anisotropy parameter. The periodic boundary condition is considered. Given the ground-state phase diagram of the XXZ at zero temperature [40], the model has three phases. In the limit $\Delta \gg 1$, the interactions in the XY plane will be ignored, thus the model should be in an antiferromagnetic phase. On the other hand, in the limit $\Delta \ll -1$, the model should be in a ferromagnetic phase. In the intermediate region, the system is in the gapless Luttinger liquid phase. These three phases are separated by two critical points (CPs). At $\Delta = 1$, we have a continuous quantum phase transition (QPT) and, at $\Delta = -1$, we have a first-order transition. At zero temperature, the quantum correlation between the first neighbor spins in the XXZ model is studied [13]. It infers that the quantum correlation between the first-neighbor spins is maximal at the critical point $\Delta = 1$ [41]. The critical point $\Delta = -1$ is not conformal and has recently attracted some attention [42–44]. It is shown that the finite-size corrections to the energy per site nontrivially vanish in the ferromagnetic $\Delta \to -1^+$ isotropic limit. The multipartite quantum nonlocality is also investigated in this model [45]. At finite temperature, the quantum correlations between the first-neighbor spins are also investigated in this model [15,46]. It is inferred that the quantum phase transitions have a decisive influence on a system's physical property not only for low temperatures, but also for sufficiently high temperatures where quantum fluctuations no longer dominate.

One of the striking effects is the dependence of the physical properties of the 1D spin-$\frac{1}{2}$ XXZ model on the direction of the applied magnetic field. It is known that adding a transverse magnetic field ($h \sum_{n=1}^{N} S_n^x$) to the XXZ model breaks the U(1) symmetry and the exact integrability is lost [47–49]. The TF induces a gap in the region $-1 < \Delta \leqslant 1$ and the ground state has the long-range spin-flop order up to a critical TF.

In the region $\Delta > 1$ ($\Delta \leqslant -1$), by applying the TF, a phase transition from the Néel (ferromagnetic) phase to a phase with saturated magnetization along field occurs at a critical TF. Moreover, a completely factorized [50] ground state may occur at a specific value of the TF, $h_f = J\sqrt{2(1 + \Delta)}$. It was shown that the entanglement of the factorized state in a TF is remarkably singled out by entanglement [51–53]. The experimental observations on the quasi-one-dimensional spin-$\frac{1}{2}$ antiferromagnet Cs$_2$CoCl$_4$ are a realization of the effect of such a TF on the low-energy behavior of a 1D XXZ model [54,55].

The paper is organized as follows: In the next section, we introduce the model and express an analytical form for the entanglement and the QD. In Sec. III, analytical results will be presented. Finally, we conclude and summarize our results in Sec. IV.

II. QUANTUM CORRELATIONS

Initially, by performing a rotation of spins around the y axis by $\pi/2$, the 1D spin-$\frac{1}{2}$ XXZ in a transverse field is transformed as [48]

$$\mathcal{H} = \sum_{n=1}^{N} \left[J\Delta S_n^x S_{n+1}^x + J\left(S_n^y S_{n+1}^y + S_n^z S_{n+1}^z \right) \right] - h \sum_{n=1}^{N} S_n^z. \tag{2}$$

At second, by applying the Jordan–Wigner transformation

$$S_n^+ = a_n^\dagger (e^{i\pi \sum_{l<n} a_l^\dagger a_l}), \quad S_n^- = (e^{-i\pi \sum_{l<n} a_l^\dagger a_l}) a_n, \tag{3}$$

$$S_n^z = a_n^\dagger a_n - \frac{1}{2}, \tag{4}$$

the Hamiltonian is mapped onto a Hamiltonian of a 1D interacting fermionic system,

$$\begin{aligned}
\mathcal{H} = {}& \frac{J(\Delta - 1)}{4} \sum_n (a_n^\dagger a_{n+1}^\dagger + \text{H.c.}) \\
& + \frac{J(\Delta + 1)}{4} \sum_n (a_n^\dagger a_{n+1} + \text{H.c.}) \\
& + J\Delta \sum_n [a_n^\dagger a_n (a_{n+1}^\dagger a_{n+1} - 1)] \\
& - h \sum_n a_n^\dagger a_n. \tag{5}
\end{aligned}$$

At third, by using Wick's theorem, the fermion interaction term is decomposed by some order parameters which are related to the two-point correlation functions as

$$\begin{aligned}
\gamma_1 &= \langle a_n^\dagger a_n \rangle, \\
\gamma_2 &= \langle a_n^\dagger a_{n+1} \rangle, \\
\gamma_3 &= \langle a_n^\dagger a_{n+1}^\dagger \rangle. \tag{6}
\end{aligned}$$

By utilizing these order parameters and performing a Fourier transformation as $a_n = \frac{1}{\sqrt{N}} \sum_k e^{-ikn} a_k$, and also Bogoliubov transformation

$$a_k = \cos(k)\alpha_k - i\sin(k)\alpha_{-k}^\dagger, \tag{7}$$

the diagonalized Hamiltonian is given by

$$\mathcal{H}_f = \sum_{k=-\pi}^{\pi} \varepsilon(k)\left(\alpha_k^\dagger \alpha_k - \frac{1}{2}\right), \tag{8}$$

where the energy spectrum is

$$\varepsilon(k) = \sqrt{a(k)^2 + b(k)^2},$$

$$a(k) = \left(\frac{J(\Delta+1)}{2} - 2\gamma_2\right)\cos(k) + (2\gamma_1 - 1)J - h,$$

$$b(k) = \left(2J\gamma_3 + \frac{J(\Delta-1)}{2}\right)\sin(k). \tag{9}$$

One should note that the following equations should be satisfied self-consistently:

$$\gamma_1 = \frac{1}{2} - \frac{1}{\pi}\int_0^\pi dk \frac{a(k)}{\varepsilon(k)}\left(\frac{1}{2} - f(k)\right),$$

$$\gamma_2 = -\frac{1}{\pi}\int_0^\pi dk \cos(k)\frac{a(k)}{\varepsilon(k)}\left(\frac{1}{2} - f(k)\right), \tag{10}$$

$$\gamma_3 = -\frac{1}{2\pi}\int_0^\pi dk \sin(k)\frac{b(k)}{\varepsilon(k)}\left(\frac{1}{2} - f(k)\right),$$

where the Fermi distribution function is $f(k) = 1/(1 + e^{\beta\varepsilon(k)})$, $\beta = \frac{1}{k_B T}$, and the Boltzmann constant is taken as $k_B = 1$. The concurrence between two spins at site i and j can be achieved from the corresponding reduced density matrix ρ_{ij}, which in the standard basis is expressed as

$$\rho_{i,j} = \begin{pmatrix} \langle P_i^\uparrow P_j^\uparrow \rangle & \langle P_i^\uparrow S_j^- \rangle & \langle S_i^- P_j^\uparrow \rangle & \langle S_i^- S_j^- \rangle \\ \langle P_i^\uparrow S_j^+ \rangle & \langle P_i^\uparrow P_j^\downarrow \rangle & \langle S_i^- S_j^+ \rangle & \langle S_i^- P_j^\downarrow \rangle \\ \langle S_i^+ P_j^\uparrow \rangle & \langle S_i^+ S_j^- \rangle & \langle P_i^\downarrow P_j^\uparrow \rangle & \langle P_i^\downarrow S_j^- \rangle \\ \langle S_i^+ S_j^+ \rangle & \langle S_i^+ P_j^\downarrow \rangle & \langle P_i^\downarrow S_j^+ \rangle & \langle P_i^\downarrow P_j^\downarrow \rangle \end{pmatrix},$$

where $P^\uparrow = \frac{1}{2} + S^z$, $P^\downarrow = \frac{1}{2} - S^z$. The brackets symbolize the thermodynamic average values at zero and finite temperature. In this literature, we introduce $S^\pm$ as $S^\pm = S^x \pm iS^y$. By applying the Jordan–Wigner transformation, the reduced

density matrix will be written as [56–59]

$$\rho_{i,j} = \begin{pmatrix} X^+ & 0 & 0 & 0 \\ 0 & Y^+ & Z^* & 0 \\ 0 & Z & Y^- & 0 \\ 0 & 0 & 0 & X^- \end{pmatrix},$$

where $X^+ = \langle n_i n_j \rangle (n_j = a_j^\dagger a_j)$, $Y^+ = \langle n_i(1 - n_j) \rangle$, $Y^- = \langle n_j(1 - n_i) \rangle$, $Z = \langle a_i^\dagger a_j \rangle$, and $X^- = \langle 1 - n_i - n_j + n_i n_j \rangle$. Thus, the concurrence is transformed into

$$C_{i,j} = \max\{0, 2(|Z| - \sqrt{X^+ X^-})\}.$$

Now, to study the quantum discord (QD), we follow Sarandy's prescription [14]. The mutual information is given as

$$\mathcal{I}(\rho_{i,j}) = S(\rho_i) + S(\rho_j) + \sum_{\alpha=0}^{3} \lambda_\alpha \log \lambda_\alpha, \tag{11}$$

where

$$S(\rho_i) = S(\rho_j) = -\left[\left(\frac{1+c_3}{2}\right)\log\left(\frac{1+c_3}{2}\right) + \left(\frac{1-c_3}{2}\right)\log\left(\frac{1-c_3}{2}\right)\right], \tag{12}$$

λ_α is the eigenvalue of $\rho_{i,j}$, and new variables are related to the elements of the density matrix as

$$c_1 = 2Z, \quad c_2 = X^+ + X^- - Y^+ - Y^-,$$

$$c_3 = X^+ - X^-. \tag{13}$$

To investigate the classical correlations between pair spins located at sites i and j, one should introduce a set of projectors for a local measurement on part $(j) = B$ given by $\{B_{k'} = V\Pi_{k'}V^\dagger\}$ where $\{\Pi_{k'} = |k'\rangle\langle k'| : k' = 0,1\}$ is the set of projectors on the computational basis $|0\rangle \equiv |\uparrow\rangle$ and $|1\rangle \equiv |\downarrow\rangle$ and $V \in \text{U}(2)$. V is parametrized as

$$V = \begin{pmatrix} \cos\frac{\theta}{2} & \sin\frac{\theta}{2}e^{-i\phi} \\ \sin\frac{\theta}{2}e^{i\phi} & -\cos\frac{\theta}{2} \end{pmatrix}, \tag{14}$$
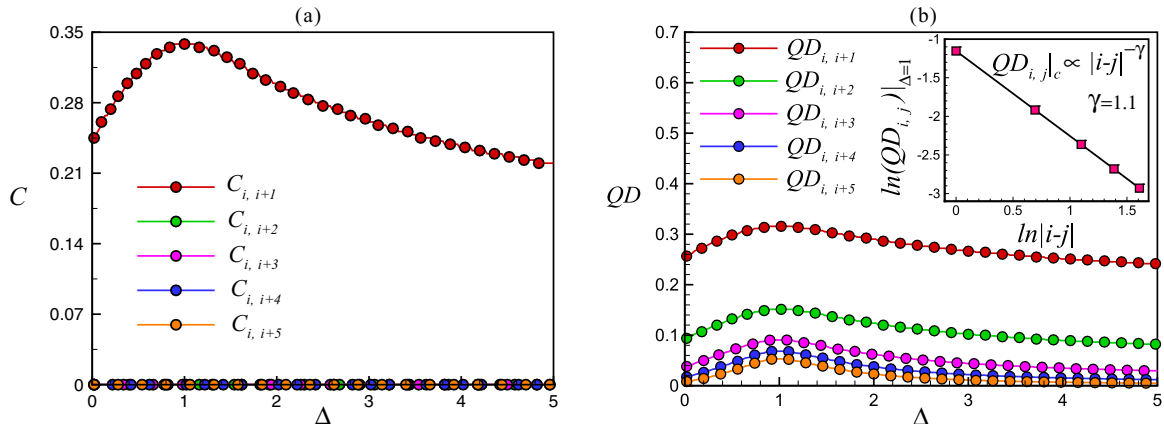
FIG. 1. (a) Entanglement of formation and (b) quantum discord between the first-, second-, third-, fourth-, and fifth-nearest neighbors as a function of anisotropy at zero temperature and zero magnetic field. Inset shows scaling behavior of quantum discord at the critical point $\Delta = 1$ in terms of distances between spins pair. Parameters are dimensionless.
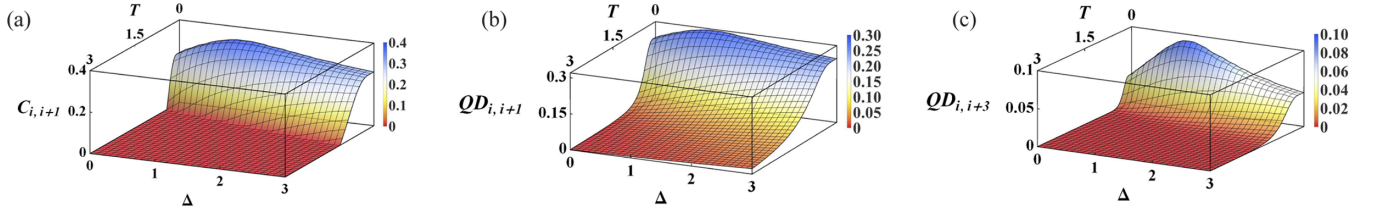
FIG. 2. The three-dimensional panorama of thermal (a) entanglement between first-nearest neighbors, (b) quantum discord between first-nearest neighbors and (c) quantum discord between second-nearest-neighbor spin pairs at zero magnetic field. Parameters are dimensionless.

where $0 \leqslant \theta \leqslant \pi$ and $0 \leqslant \phi < 2\pi$ and they can be interpreted as the azimuthal and polar angles of a qubit over the Bloch sphere. After the measurement $B_{k'}$, the physical state of the system will change to one of the following states:

$$\rho_0 = \left(\frac{I}{2} + \sum_{j=1}^{3} q_{0j} S_j\right) \otimes \left(V \Pi_0 V^\dagger\right), \quad (15)$$

$$\rho_1 = \left(\frac{I}{2} + \sum_{j=1}^{3} q_{1j} S_j\right) \otimes \left(V \Pi_1 V^\dagger\right), \quad (16)$$

where

$$q_{k'1} = (-1)^{k'} c_1 \left[\frac{\sin\theta\cos\phi}{1 + (-1)^{k'} c_3 \cos\theta}\right],$$

$$q_{k'2} = \tan\phi \, q_{k'1}, \quad (17)$$

$$q_{k'3} = (-1)^{k'} \left[\frac{c_2 \cos\theta + (-1)^{k'} c_3}{1 + (-1)^{k'} c_3 \cos\theta}\right].$$

Then, by evaluating the von Neumann entropy from Eqs. (15) and (16) and using that $S(V \Pi_0 V^\dagger) = 0$, we obtain

$$S(\rho_{k'}) = -\left(\frac{1 + \theta_{k'}}{2}\right) \log\left(\frac{1 + \theta_{k'}}{2}\right)$$
$$+ \left(\frac{1 - \theta_{k'}}{2}\right) \log\left(\frac{1 - \theta_{k'}}{2}\right), \quad (18)$$

with $\theta_{k'} = (\sum_{j=1}^{3} q_{k'j}^2)^{1/2}$. Finally, the classical correlation for the spin pair will be given by

$$\mathcal{C}(\rho_{i,j}) = \max_{\{\Pi_i^B\}} \left(S(\rho_i) - \frac{S(\rho_0) + S(\rho_1)}{2}\right.$$
$$\left. - c_3 \cos\theta \frac{S(\rho_0) - S(\rho_1)}{2}\right),$$

and the QD is determined as

$$QD = \mathcal{I}(\rho_{i,j}) - \mathcal{C}(\rho_{i,j}). \quad (19)$$

III. RESULTS

In this section, we report the results of our numerical simulations, which are based on an analytical approach of the entanglement and the QD between spin pairs.

We begin our analysis by studying the behavior of entanglement and QD as a function of the anisotropy parameter in the absence of the TF at zero temperature where the model is integrable [33]. Quantum correlations (QCs) between the first-, second-, third-, fourth-, and fifth-neighbor spins have been depicted versus Δ in Figs. 1(a) and 1(b). As seen in Fig. 1(a), only the first-neighboring spins are entangled in the whole range of the anisotropy parameter $\Delta \geqslant 0$ and are maximal at the critical point $\Delta_c = 1.0$. One can clearly see in Fig. 1(b) that the QD of the first-, second-, third-, fourth-, and fifth-neighboring pairs is nonzero and, as expected, it decreases with increasing distance between spin pairs. Also, the QD of all the first-, second-, third-, fourth-, and fifth-neighboring pairs reaches its maximum at the critical point $\Delta_c = 1.0$. A more detailed analysis shows that the QD of spin pairs at the critical point decays algebraically with distance between pairs
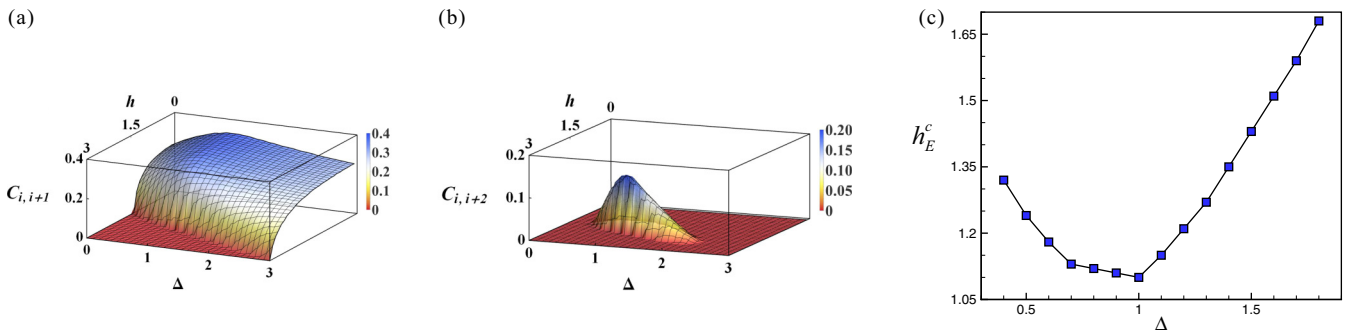
FIG. 3. Three-dimensions of entanglement as a function of magnetic field and anisotropy Δ at zero temperature between the (a) first- and (b) second-nearest-neighbor spins. (c) The critical entangled field as a function of anisotropy parameter Δ, at $T = 0$. Parameters are dimensionless.
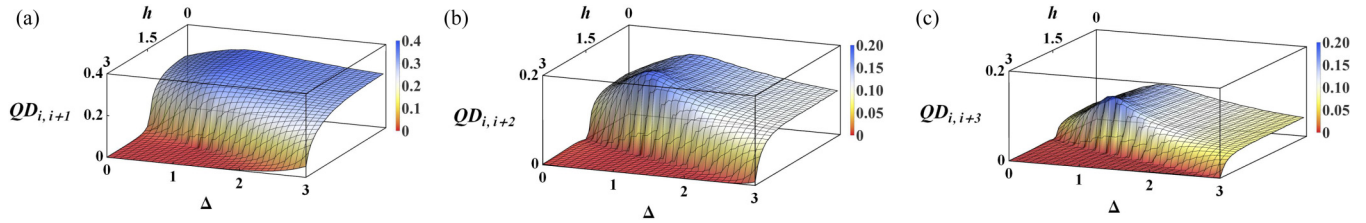
FIG. 4. Three-dimensional view of quantum discord as a function of magnetic field and anisotropy Δ at zero temperature, between the (a) first-, (b) second-, and (c) third-nearest-neighbors spins. Parameters are dimensionless.

$QD_{i,j}|_c \propto |i-j|^{-\gamma}$ with $\gamma = -1.1$ [see inset of Fig. 1(b)]. This behavior reveals that there exist long-range quantum correlations as quantified by quantum discord which decay as a function of distance in short-range magnetic interaction systems. This is in contrast with the short-ranged behavior of the pairwise entanglement.

To show whether the thermal QD (TQD) of spin pairs is able to pinpoint the critical point $\Delta_c = 1$ at finite temperature, we plot the thermal entanglement and TQD versus the anisotropy and temperature in Figs. 2(a)–2(c) for $h = 0$. The analysis shows that, while the maximum of the low-temperature thermal entanglement does not occur at the critical point $\Delta_c = 1$, the phase-transition point can be signaled by the maximum of the TQD of the spin pairs at low temperature, even for spin pairs more distant than nearest neighbors [Fig. 2(c)]. The maximum value is the result of an optimal mixing of all eigenstates in the system. Although the maximum value of the low-temperature TQD decreases as the distance between the spin pairs increases, the slope in the critical region gets more visible for far neighbors [Fig. 2(c)]. Thus, the low-temperature TQD between far neighbors can be used to characterize the zero-temperature phase transition. These results are qualitatively in agreement with the results of Ref. [15], where the exact solution of the model is presented by solving a set of nonlinear integral equations.

In addition, at high temperature, both entanglement and QD between the first-neighbor spins reduce upon increasing the temperature. As a result, the entanglement and the TQD become zero at the critical temperatures $T_c^E(\Delta)$ and $T_c^D(\Delta)$, respectively. More analysis shows that the critical temperatures, $T_c^{E,D}(\Delta)$, where quantum-classical phase transition occurs, decrease by increasing the distance between spin pairs and increase by enhancing the anisotropy parameter Δ. Moreover, an increment of temperature decreases the TQD between arbitrarily distant spin pairs and cannot create entanglement between spin pairs farther than first-nearest neighbors.

The next step is to examine how the entanglement and QD capture the QPT in the presence of a transverse field at both zero and finite temperature. To this end, we have calculated the entanglement and QD as a function of the TF and anisotropy at zero and finite temperature. A three-dimensional view of quantum entanglement between the first- and second-neighbor spins has been depicted in Figs. 3(a) and 3(b) versus h and Δ for $T = 0$.

As seen in Fig. 3(a), the entanglement between the first spin pairs remains finite up to the factorized field [$h_f = J\sqrt{2(1+\Delta)}$] and it clearly vanishes as expected for a factorized state where the ground state of the chain is exactly separable. It should be mentioned that, in Refs. [51,53], entanglement between the first-neighbor spins has been investigated through numerical approaches. It was shown that, for finite lattice size, entanglement shows a steep recovery beyond the factorized field and remains finite even in the saturated region $h > h_c$. As expected, all QCs should vanish in the saturated region. Consequently, the mean-field analytical approach shows more accurate result than the numerical method used in Refs. [51,53].

As has been shown in Fig. 1(a), only the nearest-neighbor spin pairs are entangled when the transverse magnetic field is zero, while the QD exists between spin pairs arbitrarily distant [Fig. 1(b)]. It is seen from Fig. 3(b) that the second-neighbor spin pairs become entangled in the presence of the transverse magnetic field for certain regions of parameter space. The second-neighbor spin pairs remain disentangled up to the desired critical entangled field, $h_c^E < h_f$. In other words, there is a threshold transverse field h_c^E above which the second-neighbor spins become entangled at zero temperature. The entanglement which is induced by an external magnetic field is known as the "magnetic entanglement" and was reported for longitudinal magnetic fields [13,28,59–61]. It is worthwhile to mention that the phase transition at $T = 0$ is pinpointed by a global maximum of entanglement between both
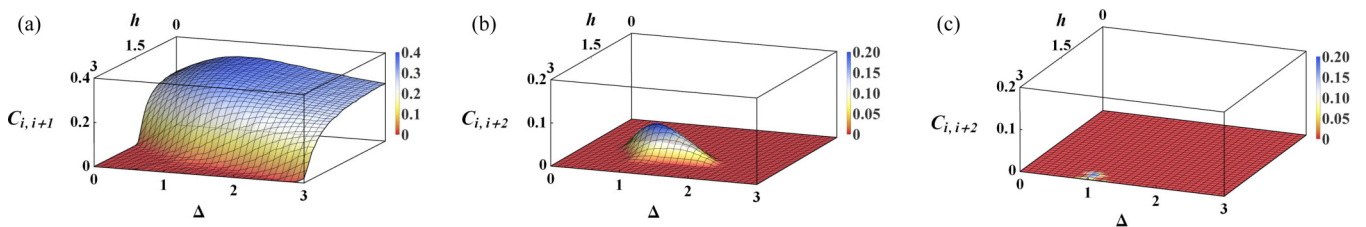
FIG. 5. Three-dimensional panorama of the entanglement as a function of magnetic field and anisotropy Δ at $T = 0.1$, between the (a) first- and (b) second-nearest-neighbors spins. (c) Three-dimensional view of the entanglement as a function of h and Δ between the second-nearest-neighbors spins at $T = 0.2$. Parameters are dimensionless.
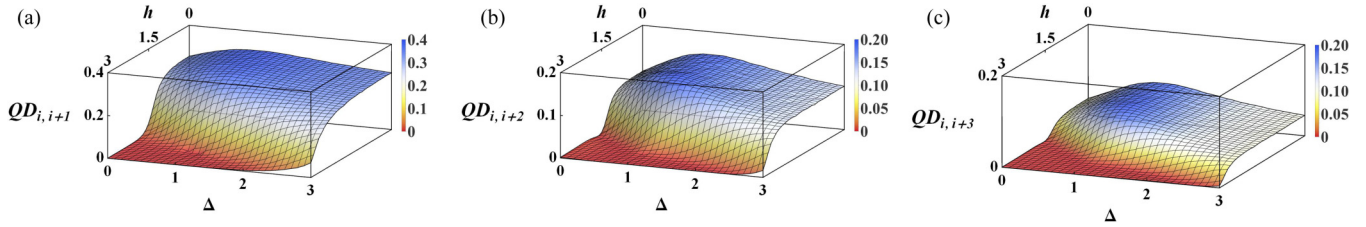
FIG. 6. Three-dimensional view of quantum discord as a function of magnetic field and anisotropy Δ at $T = 0.1$, between the (a) first-, (b) second-, and (c) third-nearest-neighbor spins. Parameters are dimensionless.

first- and second-neighbor spin pairs at the critical point $\Delta_c = 1$. However, at zero temperature the TF is incapable of creating the magnetic entanglement between spin pairs at distances beyond the next-nearest neighbors. This behavior is in contrast with the case of XXZ in a longitudinal magnetic field [59].

To find more information about the magnetic entanglement region, we calculated the critical entangled field for different values of the anisotropy with the result shown in Fig. 3(c). As expected, the magnetic field which can create entanglement between particles should have minimum strength at the critical point due to the divergence of correlation length. As seen, the critical entangled field h_E gives rise to the fingerprint of the quantum phase transition by displaying a minimum at the critical point $\Delta_c = 1.0$.

Additionally, a three-dimensional panorama of the QD between the first-, second-, and third-neighbor spin pairs at zero temperature is displayed in Figs. 4(a)–4(c) versus h and Δ. As seen, the QD between the first-, second-, and third-neighbor spins descends by the onset of the TF and vanishes at $h_{QD}^{(|i-j|)}(\Delta)$. The QD is also reserved between the third-neighbor spins in the presence of a magnetic field where pairwise entanglement is absent. We can see that the QPT is characterized by a global maximum of QD at the CP. Besides, the QD shows a cusp at the CP upon increasing the distance between the spin pairs [Fig. 4(c)]. This behavior intimates that the first derivative of the QD between spin pairs beyond the next-nearest-neighbor distance is discontinuous at $\Delta_c = 1$ and its second derivative diverges at the CP.

To investigate the effect of temperature, we plot the entanglement between first- and second-nearest-neighbor spins versus magnetic field and anisotropy at $T = 0.1$ in Figs. 5(a)–5(b). One can clearly see that, at low temperature, thermal entanglement behaves similar to the zero temperature counterpart except that its maximum does not occur at the

critical point. Moreover, the entanglement decreases as temperature increases and becomes disentangled gradually at high temperature [see Fig. 5(c)]. Our analysis also shows that the critical entangled field (h_c^E) is not a minimum in the presence of temperature. In other words, thermal entanglement is not able to detect the critical point even at low temperature. It can be clearly seen that, from Figs. 6(a)–6(c), TQD is more resistant to thermal effects than entanglement. At low temperature, the QPT is still characterized by a global maximum of QD at the CP while the cusp at the CP of TQD between far neighbors is eliminated by thermal fluctuations. In contrast to the thermal entanglement, TQD is still a better estimator of the QCP in the presence of a transverse field.

To complement our studies about the transverse field XXZ model we present the thermal behavior of the quantum correlations in the presence of the TF. It is necessary to mention that, in the saturation region, $h > h_c$, adding temperature creates neither the entanglement nor the QD. In Figs. 7(a)–7(c), we plot the thermal entanglement and TQD as a function of the magnetic field and temperature for the anisotropy parameter $\Delta = 0.5$. It is clear that there is a critical value of the field, $h_c^{(E,D)}(\Delta)$, beyond which entanglement and QD disappear at zero temperature and decline at finite temperature, $h_c^{(E,D)}(\Delta,T)$. We have found also a critical temperature $T_c^{(E,D)}(h,\Delta)$ after which entanglement and QD vanish, although there is a range of field (near to the factorized field) over which entanglement and QD can be increased by increasing the temperature. Enhancing of entanglement and QD with temperature in the presence of a magnetic field is a result of the fact that the ground state tends to be less correlated than some low-lying excited states. Thus, correlated excited states are populated by increasing the temperature, in turn leading to the net effect of an increasing of entanglement and QD. This effect gets wiped out as the temperature gets too large. This behavior is similar to the behavior of entanglement reported in Ref. [62].
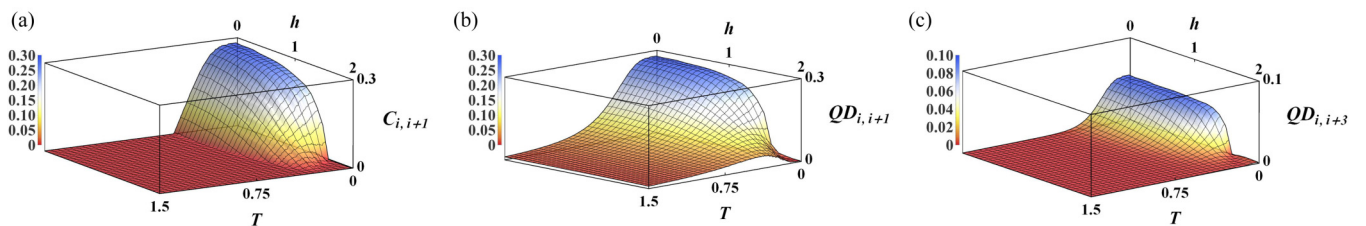
FIG. 7. (a) Thermal entanglement of formation between first-neighbor spin pairs, (b) thermal quantum discord between first-neighbor spin pairs, and (c) thermal quantum discord between third-neighbor spin pairs as a function of magnetic field and temperature for $\Delta = 0.5$. Parameters are dimensionless.

IV. CONCLUSION

We have studied the pairwise quantum correlations measured by the entanglement and the quantum discord in the thermodynamic limit of the nonintegrable XXZ spin-$\frac{1}{2}$ chain in a transverse magnetic field at zero and finite temperatures. We have obtained analytical expressions for quantum correlations for spin pairs at any distance. We have shown that the quantum discord between far neighbors is able to mark the quantum phase transition, even for distances where pairwise entanglement is absent. This is the results of the longer range of quantum correlation as quantified by quantum discord in comparison with the short-range behavior of pairwise entanglement. Concerning the thermal effect onto quantum correlations, we have shown that thermal quantum discord between neighboring pairs displays a strong distinctive behavior at the critical point that can be detected at finite temperature. This significant property of thermal quantum discord is an important tool that can be easily applied to determine quantum critical points of the systems which today's technology makes it virtually impossible to achieve the necessary T below which quantum fluctuations dominate. Moreover, the thermal quantum discord behaves more robust than the thermal entanglement as the temperature is increased. We have also shown that the transverse magnetic field creates the magnetic entanglement between the second-neighbor spins in a narrow region under the factorized field. Remarkably, we show that quantum correlations can be increased with temperature in the presence of the magnetic field for certain regions of parameter space.

[1] M. Vojta, Rep. Prog. Phys. **66**, 2069 (2003).

[2] S. Sachdev, *Quantum Phase Transitions* (Cambridge University Press, 2001).

[3] J. Preskill, J. Mod. Opt. **47**, 127 (2000).

[4] E. Schrödinger, Math. Proc. Cambridge Philos. Soc. **31**, 555 (1935).

[5] R. Horodecki, P. Horodecki, M. Horodecki, and K. Horodecki, Rev. Mod. Phys. **81**, 865 (2009).

[6] S. Hill and W. K. Wootters, Phys. Rev. Lett. **78**, 5022 (1997).

[7] W. K. Wootters, Phys. Rev. Lett. **80**, 2245 (1998).

[8] K. Modi, A. Brodutch, H. Cable, T. Paterek, and V. Vedral, Rev. Mod. Phys. **84**, 1655 (2012).

[9] H. Ollivier and W. H. Zurek, Phys. Rev. Lett. **88**, 017901 (2001).

[10] J. Oppenheim, M. Horodecki, P. Horodecki, and R. Horodecki, Phys. Rev. Lett. **89**, 180402 (2002).

[11] A. Datta, A. Shaji, and C. M. Caves, Phys. Rev. Lett. **100**, 050502 (2008).

[12] B. P. Lanyon, M. Barbieri, M. P. Almeida, and A. G. White, Phys. Rev. Lett. **101**, 200501 (2008).

[13] R. Dillenschneider, Phys. Rev. B **78**, 224413 (2008).

[14] M. S. Sarandy, Phys. Rev. A **80**, 022108 (2009).

[15] T. Werlang, C. Trippe, G. A. P. Ribeiro, and G. Rigolin, Phys. Rev. Lett. **105**, 095702 (2010).

[16] Y.-X. Chen and S.-W. Li, Phys. Rev. A **81**, 032120 (2010).

[17] R. Jafari, Phys. Rev. A **82**, 052317 (2010).

[18] B. Tomasello, D. Rossini, A. Hamma, and L. Amico, Europhys. Lett. **96**, 27002 (2011).

[19] B. Tomasello, D. Rossini, A. Hamma, and L. Amico, Int. J. Mod. Phys. B **26**, 1243002 (2012).

[20] R. Jafari and A. Akbari, Europhys. Lett. **111**, 10007 (2015).

[21] J. Maziero, L. C. Céleri, R. M. Serra, and V. Vedral, Phys. Rev. A **80**, 044102 (2009).

[22] A. Shabani and D. A. Lidar, Phys. Rev. Lett. **102**, 100402 (2009).

[23] T. Werlang, S. Souza, F. F. Fanchini, and C. J. Villas Boas, Phys. Rev. A **80**, 024103 (2009).

[24] K. Modi, T. Paterek, W. Son, V. Vedral, and M. Williamson, Phys. Rev. Lett. **104**, 080501 (2010).

[25] K. Brádler, M. M. Wilde, S. Vinjanampathy, and D. B. Uskov, Phys. Rev. A **82**, 062310 (2010).

[26] A. Datta, Phys. Rev. A **80**, 052304 (2009).

[27] L. C. Céleri, A. G. S. Landulfo, R. M. Serra, and G. E. A. Matsas, Phys. Rev. A **81**, 062130 (2010).

[28] J. Maziero, H. C. Guzman, L. C. Céleri, M. S. Sarandy, and R. M. Serra, Phys. Rev. A **82**, 012106 (2010).

[29] J. Maziero, L. Céleri, R. Serra, and M. Sarandy, Phys. Lett. A **376**, 1540 (2012).

[30] S. Campbell, J. Richens, N. L. Gullo, and T. Busch, Phys. Rev. A **88**, 062305 (2013).

[31] X.-D. Tan, X.-L. Wang, S.-S. Huang, and B.-Q. Jin, Int. J. Theor. Phys. **53**, 91 (2014).

[32] D. Sadhukhan, S. S. Roy, D. Rakshit, R. Prabhu, A. Sen(De), and U. Sen, Phys. Rev. E **93**, 012131 (2016).

[33] A. Klümper, Z. Phys. B: Condens. Matter **91**, 507 (1993).

[34] P. Hauke, C. Hempel, P. Zoller, R. Blatt, and C. F. Roos, Nature (London) **511**, 202 (2014).

[35] R. Toskovic, R. van den Berg, A. Spinelli, I. S. Eliens, B. van den Toorn, B. Bryant, J.-S. Caux, and A. F. Otte, Nat. Phys. **12**, 656 (2016).

[36] U. Glaser, H. Büttner, and H. Fehske, Phys. Rev. A **68**, 032318 (2003).

[37] D. Loss and D. P. DiVincenzo, Phys. Rev. A **57**, 120 (1998).

[38] G. Burkard, D. Loss, and D. P. DiVincenzo, Phys. Rev. B **59**, 2070 (1999).

[39] J.-S. Caux, F. H. L. Essler, and U. Löw, Phys. Rev. B **68**, 134431 (2003).

[40] M. Takahashi, *Thermodynamics of One-Dimensional Solvable Models* (Cambridge University Press, 1999).

[41] J.-M. Cai, Z.-W. Zhou, and G.-C. Guo, Phys. Lett. A **352**, 196 (2006).

[42] L. Banchi, F. Colomo, and P. Verrucchi, Phys. Rev. A **80**, 022341 (2009).

[43] V. Alba, K. Saha, and M. Haque, J. Stat. Mech.: Theory Exp. (2013) P10018.

[44] J. Stasińska, B. Rogers, M. Paternostro, G. De Chiara, and A. Sanpera, Phys. Rev. A **89**, 032330 (2014).

[45] Z.-Y. Sun, S. Liu, H.-L. Huang, D. Zhang, Y.-Y. Wu, J. Xu, B.-F. Zhan, H.-G. Cheng, C.-B. Duan, and B. Wang, Phys. Rev. A **90**, 062129 (2014).

[46] T. Werlang, G. A. P. Ribeiro, and G. Rigolin, Phys. Rev. A **83**, 062334 (2011).

[47] J. Kurmann, H. Thomas, and G. Müller, Phys. A (Amsterdam, Neth.) **112**, 235 (1982).

[48] D. V. Dmitriev, V. Y. Krivnov, and A. A. Ovchinnikov, Phys. Rev. B **65**, 172409 (2002).

[49] A. Langari and S. Mahdavifar, Phys. Rev. B **73**, 054410 (2006).

[50] S. M. Giampaolo, G. Adesso, and F. Illuminati, Phys. Rev. Lett. **100**, 197201 (2008).

[51] T. Roscilde, P. Verrucchi, A. Fubini, S. Haas, and V. Tognetti, Phys. Rev. Lett. **93**, 167203 (2004).

[52] J. Abouie, A. Langari, and M. Siahatgar, J. Phys.: Condens. Matter **22**, 216008 (2010).

[53] L. Amico, D. Rossini, A. Hamma, and V. E. Korepin, Phys. Rev. Lett. **108**, 240503 (2012).

[54] M. Kenzelmann, R. Coldea, D. A. Tennant, D. Visser, M. Hofmann, P. Smeibidl, and Z. Tylczynski, Phys. Rev. B **65**, 144432 (2002).

[55] O. Breunig, M. Garst, E. Sela, B. Buldmann, P. Becker, L. Bohatý, R. Müller, and T. Lorenz, Phys. Rev. Lett. **111**, 187202 (2013).

[56] S.-S. Gong and G. Su, Phys. Rev. A **80**, 012323 (2009).

[57] E. Mehran, S. Mahdavifar, and R. Jafari, Phys. Rev. A **89**, 042306 (2014).

[58] M. Soltani, J. Vahedi, and S. Mahdavifar, Phys. A (Amsterdam, Neth.) **416**, 321 (2014).

[59] F. K. Fumani, S. Nemati, S. Mahdavifar, and A. H. Darooneh, Phys. A (Amsterdam, Neth.) **445**, 256 (2016).

[60] H. Yano and H. Nishimori, Prog. Theor. Phys. Suppl. **157**, 164 (2005).

[61] Y. Huang, Phys. Rev. B **89**, 054410 (2014).

[62] M. C. Arnesen, S. Bose, and V. Vedral, Phys. Rev. Lett. **87**, 017901 (2001).